Contribution from the Laboratory for Molecular Structure and Bonding and the Department of Chemistry, Texas A&M University, College Station, Texas 77843, and Department of Chemistry, The Ohio State University, Columbus, Ohio 43210

Ground-State Electronic Structures and Other Electronic Properties of the Octahedral and Oligooctahedral Ruthenium Complexes Hexachlororuthenium(III), Nonachlorodiruthenium(III), and Dodecachlorotriruthenium(II,2III)

BRUCE E. BURSTEN,*[1a] F. ALBERT COTTON,*[1b] and ANNE FANG[1b]

Received November 24, 1982

The ground-state electronic structures and electronic spectra of the anions $[RuCl_6]^{3-}$, $[Ru_2Cl_9]^{3-}$, and $[Ru_3Cl_{12}]^{4-}$, which have octahedral (O_h), bioctahedral (D_{3h}), and trioctahedral (D_{3d}) structures, have been calculated by the SCF-Xα-SW method. The Fenske–Hall method has also been applied to these anions, giving results in qualitative accord with those of the SCF-Xα-SW method. The calculated results are in satisfactory accord with the observed electronic absorption spectra of the $[RuCl_6]^{3-}$ and $[Ru_2Cl_9]^{3-}$ ions. In the $[Ru_2Cl_9]^{3-}$ ion the highest filled and lowest empty MO's are derived mainly from metal atom d orbitals and it is found to have an upper electron configuration $...a_1'^2e'^4e''^4$, in which the e'' and e' electrons make essentially no net contribution to the Ru–Ru bonding; there is a net single (σ) bond between the metal atoms due to the occupied a_1' orbital. In the $[Ru_3Cl_{12}]^{3-}$ ion the highest filled orbitals are again derived mainly from metal atom d orbitals. Again there is only a net σ contribution to the metal–metal bonding such that a bond order of 0.5 can be formally assigned. In both of the polynuclear ions the atomic d orbitals form subsets with σ, π, and δ character under purely axial symmetry. However, there is very extensive mixing of the π and δ ($d_{xz,yz}$ and d_{xy,x^2-y^2}) types in the actual D_{3h} and D_{3d} symmetries imposed by the sets of chlorine atoms.

Introduction

The nature of the interactions between metal atoms in adjacent octahedra that share a face is a subject of fundamental interest. These interactions have often been studied in the past in the context of the confacial bioctahedron, especially in those of the type $[M_2X_9]^{n-}$ where all ligands are the same and the symmetry is high (D_{3h}) as shown in Figure 1a. The metal-to-metal interaction is a function of (1) the number of metal d electrons, (2) the row of the periodic table from which the metal comes, (3) the size of the anion, X^-, and (4) even the identity of the cations with which the anions are packed. These metal-to-metal interactions range from those which involve little or no direct metal–metal (M–M) bonding to those in which there are M–M bonds of appreciable strength. These trends are well represented in the $[M_2X_9]^{3-}$ ions formed by the group 6 metals, Cr, Mo, W, with either Cl^- or Br^- ligands. For the chloro species, structural,[2] magnetic,[3a,4] and spectroscopic[3,5,6] evidence clearly shows that for $[Cr_2Cl_9]^{3-}$ there is no bonding between the metal atoms and only a weak coupling between the Cr^{III} ions. A similar situation but with stronger coupling has recently been shown to exist in the $[Ti_2Cl_9]^{3-}$ ion.[7] In the $[Mo_2Cl_9]^{3-}$ ion, by the same criteria, there is weak to medium Mo–Mo bonding[8-10] while in the $[W_2Cl_9]^{3-}$ ion there is strong W–W bonding.[11-13] The change from $[Mo_2Cl_9]^{3-}$ to $[Mo_2Br_9]^{3-}$ causes the Mo–Mo bonding to become considerably weaker.[8,9]

In these laboratories we have been chiefly interested in strong M–M bonding (rather than weak interactions) in a variety of structural contexts, including structures made up of octahedra sharing edges[14] or faces.[2] Several years ago we discovered and structurally characterized for the first time a linear trinuclear structure of the type shown in Figure 1b, namely, the $[Ru_3Cl_{12}]^{4-}$ ion.[15] The structural results suggested that direct Ru–Ru bonds might be present. More recently the preparation and structural characterization of $Cs_3Ru_2Cl_9$ have been reported by J. Darriet[16] and here the structural and magnetic properties clearly suggest the existence of a strong direct Ru–Ru bond.

In this paper we report the results of a theoretical study of both of these ruthenium species, using the SCF-Xα-SW method.[17] This work was done to obtain a detailed picture of the bonding, especially the Ru–Ru bonding, in these related species. In addition, we have also treated the $[RuCl_6]^{3-}$ ion. The trinuclear anion may be formally described as a Ru^{III}–Ru^{II}–Ru^{III} system and the dinuclear anion as a Ru^{III}–Ru^{III} system. Alternatively, they could be described, prior to Ru–Ru bond formation, as d^5–d^6–d^5 and d^5–d^5 systems. In addition to the calculations, we have also attempted some preliminary spectroscopic measurements.

Procedures

Computations. Coordinates for the three anions were taken from experimental structural studies and idealized to O_h, D_{3h}, and D_{3d} symmetry for $[RuCl_6]^{3-}$, $[Ru_2Cl_9]^{3-}$, and $[Ru_3Cl_{12}]^{4-}$, respectively. The α exchange parameters for Cl and Ru were taken from the tabulations of Schwarz.[18] In each case, an initial molecular charge density and potential were constructed from a superposition of Herman–Skillman atomic charge densities for Ru^+ and Cl^{n-}, where n was determined by the charge and composition of the complex. In each case a Watson sphere was used to simulate the effect of surrounding counterions in the lattice. Sphere radii were chosen according to Norman's procedure.[19] Details are summarized in Table I. In

(1) (a) The Ohio State University. (b) Texas A&M University.
(2) Cotton, F. A.; Ucko, D. A. *Inorg. Chim. Acta* **1972**, *6*, 161.
(3) (a) Kahn, O.; Briat, B. *Chem. Phys. Lett.* **1975**, *32*, 376. (b) Briat, B.; Russel, M. F.; Rivoal, J. C.; Chapelle, J. P.; Kahn, O. *Mol. Phys.* **1977**, *34*, 1545.
(4) Beswick, J. C.; Dugdale, D. E. *J. Phys. C* **1973**, *6*, 3326.
(5) Dubicki, L.; Tanabe, Y. *Mol. Phys.* **1977**, *34*, 1531.
(6) Johnstone, I. W.; Maxwell, K. J.; Stevens, K. W. H. *J. Phys. C* **1981**, *14*, 1297.
(7) Briat, B.; Kahn, O.; Morgenstein-Badarau, I.; Rivoal, J. C. *Inorg. Chem.* **1981**, *20*, 4193.
(8) Grey, I. E.; Smith, P. W. *Aust. J. Chem.* **1971**, *24*, 73.
(9) (a) Saillant, R.; Hayden, J. L.; Wentworth, R. A. D. *Inorg. Chem.* **1967**, *6*, 1497. (b) Saillant, R.; Wentworth, R. A. D. *Ibid.* **1969**, *8*, 1226. (c) Saillant, R.; Jackson, R. B.; Streib, W. E.; Folting, K.; Wentworth, R. A. D. *Ibid.* **1971**, *10*, 1453.
(10) Ginsberg, A. P. *J. Am. Chem. Soc.* **1980**, *102*, 111.
(11) Watson, W. H., Jr.; Waser, J. *Acta Crystallogr.* **1958**, *11*, 689.
(12) Smith, P. W.; Wedd, A. G. *J. Chem. Soc. A* **1970**, 2447.
(13) Zeigler, R. J.; Risen, W. M., Jr. *Inorg. Chem.* **1972**, *11*, 2796.
(14) Anderson, L. B.; Cotton, F. A.; DeMarco, D.; Fang, A.; Ilsley, W. H.; Kolthammer, B. W. S.; Walton, R. A. *J. Am. Chem. Soc.* **1981**, *103*, 5078.
(15) Bino, A.; Cotton, F. A. *J. Am. Chem. Soc.* **1980**, *102*, 608.
(16) Darriet, J. *Rev. Chim. Miner.* **1981**, *18*, 27.
(17) (a) Johnson, K. H. *Annu. Rev. Phys. Chem.* **1975**, *26*, 39. (b) For further references and details of how the method was applied in the present instances, see: Cotton, F. A.; Hubbard, J. L.; Lichtenberger, D. L.; Shim, I. *J. Am. Chem. Soc.* **1982**, *104*, 679.
(18) Schwarz, L. *Phys. Rev. B: Solid State* **1972**, *5*, 2466; *Theor. Chim. Acta* **1974**, *34*, 225.

0020-1669/83/1322-2127$01.50/0

Table I. Input Parameters for the Calculations

ion	bond lengths, Å		bond angles, deg		sphere radii, au: atomic		sphere radii, au: outer	Watson sphere: radius, au	Watson sphere: charge
$[RuCl_6]^{3-}$	Ru-Cl	2.369	all	90	Ru	2.51501	7.09072	8.09072	4+
					Cl	2.61330			
$[Ru_2Cl_9]^{3-}$	Ru-Ru	2.725	$Ru-Ru-Cl_b$	55.25	Ru	2.5012	8.8622	9.8622	5+
	$Ru-Cl_b$	2.391	$Ru-Ru-Cl_t$	125.04	Cl_b	2.5276			
	$Ru-Cl_t$	2.332			Cl_t	2.6109			
$[Ru_3Cl_{12}]^{4-}$	Ru-Ru	2.805	$Ru-Ru-Cl_b$	53.8	Ru_1[a]	2.5111	11.3078	12.3078	6+
	$Ru-Cl_b$	2.378	$Ru-Ru-Cl_t$	124.8	Ru_2[a]	2.5168			
	$Ru-Cl_t$	2.369			Cl_b	2.5150			
					Cl_t	2.6332			

[a] Ru_1 is the central Ru atom; Ru_2 denotes the outer Ru atoms.

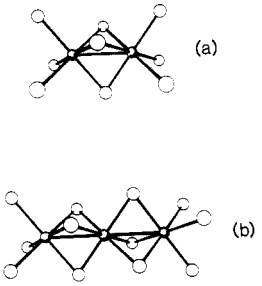

Figure 1. The confacial bioctahedron structure (a) and the linear confacial trioctahedron structure (b), discussed in this paper.

each case the coordinate system was placed with the origin at the center of the molecule. The z axis was directed along a Ru–Cl bond for $[RuCl_6]^{3-}$ and along the 3-fold axis of the molecule for $[Ru_2Cl_9]^{3-}$ and $[Ru_3Cl_{12}]^{4-}$.

Schwarz's[18] α_{HF} atomic exchange parameters were used with α values 0.702 50 for Ru and 0.723 25 for Cl atoms. A valence-electron weighted average of the atomic α values was used for the intersphere and outer-sphere regions.

The atomic spheres were allowed to overlap, and their radii were chosen as 89% of the atomic number radii. The outer-sphere radius was made tangential to the outmost atomic sphere.

The symmetry-adapted linear combinations of atomic orbitals included s, p, and d spherical harmonics on the Ru atoms, s and p on the Cl atoms. On the outer sphere, spherical harmonics up through $l = 5$ were included.

The SCF calculations were started with use of a 5% mixing of the new potential into the old potential. This percentage was gradually raised to 25%. The SCF calculations were considered to be converged when the shift in potential was less than 0.001 Ry and in valence energy levels less than 0.0001 Ry. No relativistic corrections were made since our previous experience[17b] suggests that they would be very small.

Electronic Spectrum of $[Ru_2Cl_9]^{3-}$. The compound $Cs_3Ru_2Cl_9$ is intensely colored. The crystals appear almost black by reflected light but are seen by transmitted light to be red. Attempts in this laboratory to measure the spectrum by transmission of light through powder samples suspended in mineral oil gave poor results because of reflective scattering. Through the courtesy of Dr. Douglas Carlson, Argonne National Laboratory, the photoacoustic spectrum, which was consistent with but superior to the transmission spectrum, was obtained. A Princeton Applied Research photoacoustic spectrometer was used. The results are as follows, where all features listed had intensities that differed by less (on an arbitrary scale) than a factor of 2: 18 000 (sh), 22 700, 25 000 (sh), 41 000 cm^{-1}.

Results

The $[RuCl_6]^{3-}$ Ion. A preliminary SCF–Xα–SW calculation was carried out on this open-shell species (t_{2g}^5) to see how its ground-state electronic structure would relate to those of the bioctahedral and trioctahedral species that are our chief interest here. The calculated orbital energies are shown in Figure 2. The arrangement is a simple one and is in accord with

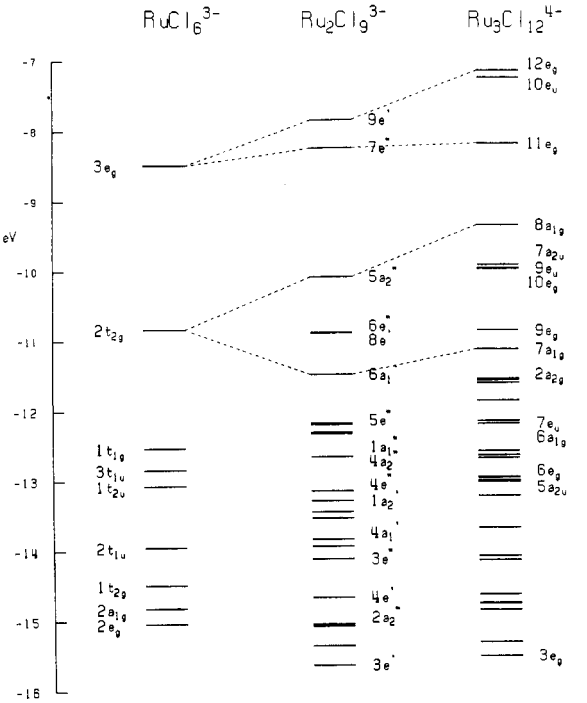

Figure 2. Ground-state orbital energies calculated for the three species $[RuCl_6]^{3-}$, $[Ru_2Cl_9]^{3-}$, and $[Ru_3Cl_{12}]^{4-}$. Dashed lines trace the participation of the π and σ types (t_{2g} and e_g, respectively) of d orbitals in the single octahedron as the oligomers are built up.

expectation. Between −15.2 and −12.6 eV we find all of the molecular orbitals that arise mainly from chlorine atom 3p atomic orbitals. The $2e_g$, $2a_{1g}$, and $2t_{1u}$ orbitals are the metal–chlorine σ-bonding orbitals, while the remaining ones, $1t_{2g}$, $1t_{2u}$, $3t_{1u}$, and $1t_{1g}$ are π-type orbitals. The last three of these, lying in the range −12.6 to −13.2 eV, are essentially pure chlorine lone-pair orbitals. The $1t_{2g}$ orbital is lowered in energy because there is an interaction with the metal 4d orbitals of t_{2g} symmetry; in effect there is significant Ru–Cl π interaction.

The HOMO is the $2t_{2g}$ orbital, which contains five electrons, and the LUMO is the $3e_g$ orbital. There have been previous indications[20] that the SCF–Xα–SW method can give fairly reliable estimates of d-orbital splittings in octahedral complexes; we wanted to see if that would be the case here. Accordingly, some excitation energies were calculated in spin-restricted form for the $[RuCl_6]^{3-}$ ion. The values thus obtained are the weighted averages of those for doublet and quartet excited states, and no corrections for relaxation effects have been made. We predict the "ligand field transition", $2t_{2g} \rightarrow 3e_g$, to be at 19 200 cm^{-1}, which is in quite good agreement with the observed value[21] of 20 500 cm^{-1}. The three allowed

(19) Norman, J. G., Jr. *Mol. Phys.* **1976**, *31*, 1191.

(20) Aizman, A.; Case, D. A. *Inorg. Chem.* **1981**, *20*, 528.

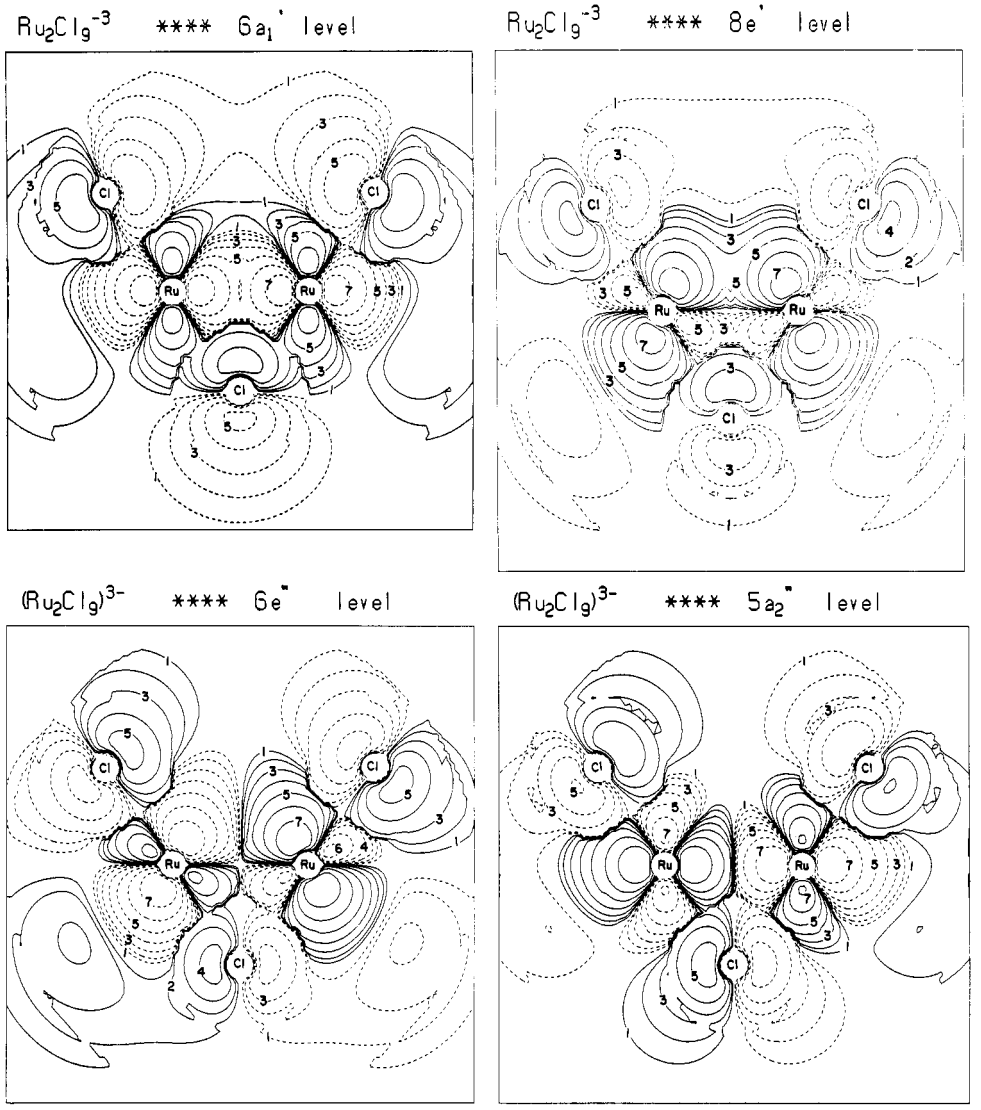

Figure 3. Contour diagrams for the three highest occupied ($6a_1'$, $8e'$, $6e''$) and lowest unoccupied ($5a_2''$) molecular orbitals of the $[Ru_2Cl_9]^{3-}$ ion. Solid and broken lines indicate opposite signs of the wave function. The lowest contour value (1) is 0.0050 e/au^3, and adjacent contours differ by a factor of 2. This code applies to all other contour plots presented in this report.

charge-transfer transitions, $3t_{1u} \rightarrow 2t_{2g}$, $1t_{2u} \rightarrow 2t_{2g}$, and $2t_{1u} \rightarrow 2t_{2g}$, are predicted to occur between 20 000 and 30 000 cm^{-1}, while the spectrum shows strong bands that may presumably be so assigned between 26 000 and 33 000 cm^{-1}.

The $[Ru_2Cl_9]^{3-}$ Ion. The results of the SCF-Xα-SW calculation are presented in Table II and in Figures 2 and 3. Table II gives a list of the occupied molecular orbitals formed from chlorine 3p orbitals and ruthenium orbitals outside the krypton core, as well as the five lowest virtual orbitals.

The three highest occupied MO's are predominantly metal based, and the metal atom contributions are of predominantly d-orbital character. The $6a_1'$ wave function is shown in Figure 3. It is clear that it is made up mainly of the d_{z^2} orbitals of the two metal atoms and that it provides a σ bond between the metal atoms. It is essentially nonbonding with respect to the bridging Cl atoms and somewhat π-antibonding toward the terminal Cl atoms. The contours of one of the $8e'$ orbitals are shown in Figure 3, from which it is clear that these serve to form a pair of π bonds between the metal atoms. They, like the $6a_1'$ orbital, are essentially nonbonding toward the bridging Cl atoms and somewhat π antibonding toward the terminal Cl atoms. The $6e''$ orbital (Figure 3), the HOMO, is similar in character to the $8e'$ orbital, but it is Ru-Ru antibonding. Thus, the net Ru-Ru bond order in $[Ru_2Cl_9]^{3-}$ is approximately unity due to the electron pair occupying the σ-type $6a_1'$ orbital. The bonding and antibonding effects of the electrons occupying the $8e'$ and $6e''$ orbitals appear to mutually offset each other to a good approximation.

The LUMO is the $5a_2''$ orbital. As the contour diagram, Figure 3, shows, it has σ antibonding character with respect to the Ru-Ru interaction. It is also antibonding with respect to all Ru-Cl interactions.

Between -12.2 eV (the $5e''$ orbital) and -15.6 eV (the $3e'$ orbital) we find molecular orbitals formed mainly from the 3p orbitals of the chlorine atoms. These filled orbitals contain a total of 27 electron pairs and comprise both the Ru-Cl bonding orbitals and the chlorine atom lone-pair orbitals.

The electronic transitions that might be expected below 50 000 cm^{-1} are listed in Table III, and these may be compared with the experimental data presented in Procedures. The allowed transitions at ca. 6000 and 11 000 cm^{-1} were not within the range of observation. The group of allowed bands between about 20 000 and 25 000 cm^{-1} may correspond with the broad absorption with shoulders or maxima between 18 000 and 25 000 cm^{-1}. Transitions predicted at ca. 29 000 and 34 000 cm^{-1} do not correspond to any observed maxima, but the observed spectrum in this region, though featureless, has high intensity. The predicted transition at 42 500 cm^{-1} might account for the observed maximum at ca. 41 000. The transitions

(21) (a) Hartmann, H.; Buschbeck, C. *Z. Phys. Chem. (Wiesbaden)* **1957**, *11*, 120. (b) Jørgensen, C. K. *Acta Chem. Scand.* **1956**, *10*, 518.

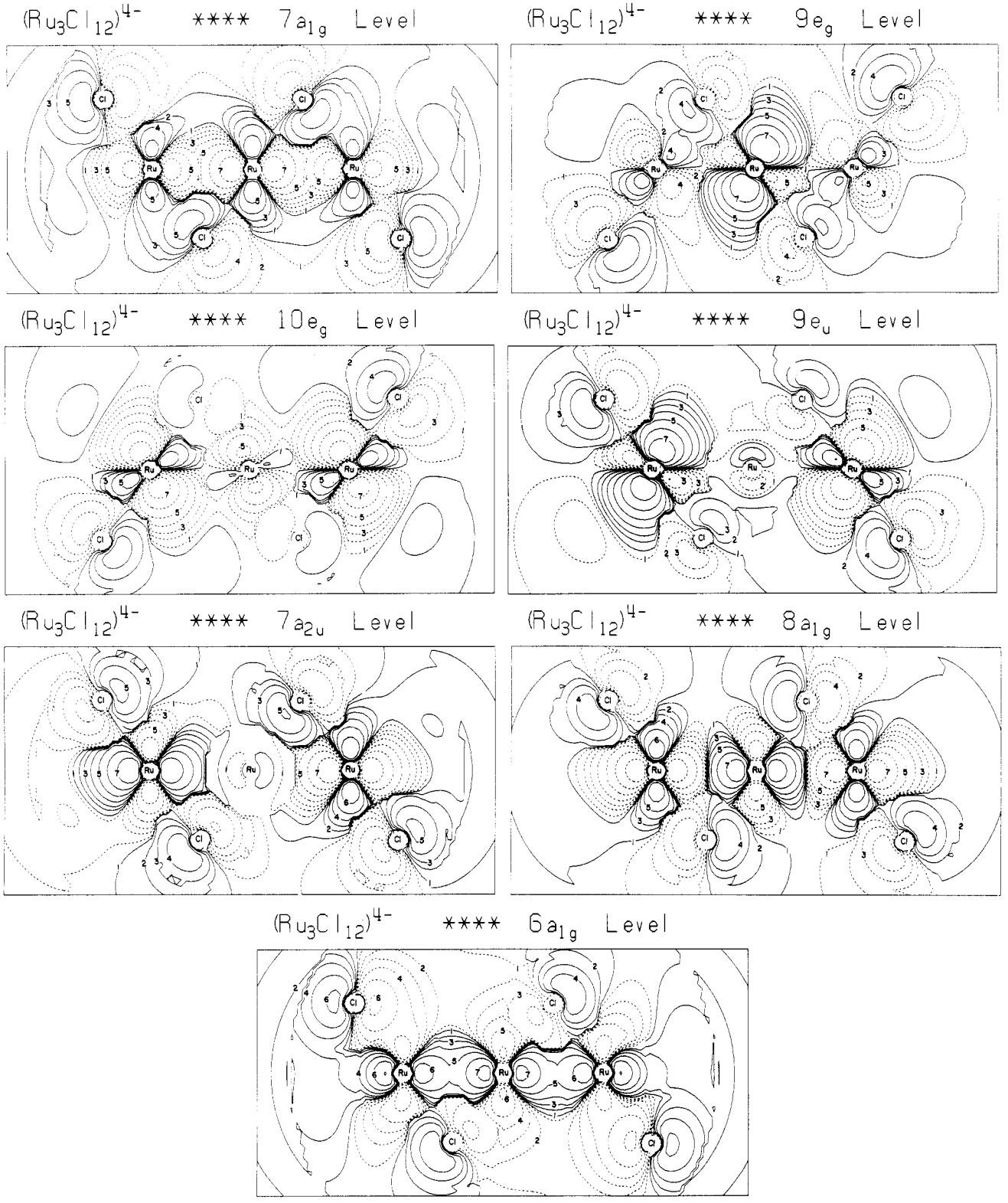

Figure 4. Contour diagrams for the five highest occupied ($7a_{1g}$, $9e_g$, $10e_g$, $9e_u$, $7a_{2u}$) and lowest unoccupied ($8a_{1g}$) molecular orbitals of the $[Ru_3Cl_{12}]^{3-}$ ion. The $6a_{1g}$ orbital, which contributes to Ru–Ru bonding, is also shown.

predicted for ca. 46 000 and 50 000 cm^{-1} are out of range of the recorded spectrum. In summary, the observed spectrum is not at all inconsistent with that predicted, but because of the poor resolution, this does not constitute a firm validation of the theoretical results.

The $[Ru_3Cl_{12}]^{4-}$ Ion. As may be seen in Figure 2 and Table IV, the highest five filled molecular orbitals have predominantly metal atom d-orbital provenance, whereas all molecular orbitals below this have predominantly (in many cases, exclusively) chlorine 3p orbital character. These latter orbitals, occupied by a total of 36 electron pairs, are either Ru–Cl bonding orbitals or chlorine lone-pair orbitals.

Let us now examine the top five filled molecular orbitals. The HOMO is the $7a_{2u}$ orbital, which is nonbonding and consists almost entirely of the d_{z^2} orbitals of the two outer ruthenium atoms. The $9e_u$ and $10e_g$ orbitals are also essentially nonbonding in all respects and are very similar to each other, as shown in Figure 4. Here again they are made up almost entirely of d orbitals on the outer ruthenium atoms. The $9e_g$ orbital, on the other hand, is largely localized on the central

Table II. Upper Valence Molecular Orbitals of $[Ru_2Cl_9]^{3-}$

level[a]	energy, eV	% contribn[b] Ru	Cl_b	Cl_t	INT	OUT	% Ru angular contribn[c] s	p	d
10e'	−5.5835	0	3	3	47	47			
$7a_1'$	−6.0355	1	2	2	53	42			
9e'	−7.8222	55	16	18	9	2			100
7e''	−8.2177	58	10	23	7	2			100
$5a_2''$	−10.0641	79	7	8	6	0			100
6e''	−10.8580	73	1	18	7	0			100
8e'	−10.8657	68	9	14	8	0			100
$6a_1'$	−11.4639	54	7	29	9	1			100
5e'	−12.1877	0	10	78	10	1			
$2a_2'$	−12.2056	0	9	80	10	1			
7e'	−12.3220	0	6	81	11	1			
$1a_1''$	−12.3294	0	0	87	12	1			
$4a_2''$	−12.3397	1	31	57	8	2			
6e'	−12.6721	3	39	46	10	1			
4e''	−13.1641	12	15	60	12	1		10	90
$1a_2'$	−13.3031	0	77	8	14	0			
5e'	−13.4603	8	20	59	12	1			
$5a_1'$	−13.5472	20	6	64	7	2	10	22	68
$4a_1'$	−13.8513	18	11	56	15	1		9	91
$3a_2''$	−13.9493	12	2	72	13	1	16	21	63
3e''	−14.1261	17	11	59	11	1		19	81
4e'	−14.6816	20	43	20	16	0		4	96
$2a_2''$	−15.0639	15	44	27	13	1	52		48
2e''	−15.0947	34	38	21	6	1			100
$3a_1'$	−15.3668	20	55	13	11	0	55	7	38
3e'	−15.6468	36	40	19	4	0			100

[a] The HOMO is the 6e'' level. [b] Abbreviations for charge distributions: INT = intersphere; OUT = outer sphere. [c] Listed only for levels with 10% or more Ru contributions.

Table III. Calculated Transition Energies for $[Ru_2Cl_9]^{3-}$

orbital transition	dipole[a]	transition energies eV	cm^{-1}
$6e'' \rightarrow 5a_2''$	a, xy	0.8018	6 467
$8e' \rightarrow 5a_2''$	f	0.8099	6 532
$6a_1' \rightarrow 5a_2''$	a, z	1.4440	11 647
$5e'' \rightarrow 5a_2''$	a, xy	2.5612	20 657
$6e'' \rightarrow 7e''$	a, xy	2.6543	21 408
$8e' \rightarrow 7e''$	a, z	2.6555	21 414
$8e' \rightarrow 9e'$	a, xy	3.0542	24 634
$6e'' \rightarrow 9e'$	a, z	3.0607	24 686
$6a_1' \rightarrow 7e''$	f	3.2527	26 235
$6a_1' \rightarrow 9e'$	a, xy	3.6531	29 464
$5e'' \rightarrow 7e''$	a, xy	4.2196	34 033
$8e' \rightarrow 7a_1'$	a, xy	5.2717	42 519
$6e'' \rightarrow 7a_1'$	f	5.2951	42 708
$8e' \rightarrow 10e'$	a, xy	5.7150	46 094
$6e'' \rightarrow 10e'$	a, z	5.7477	46 358
$6a_1' \rightarrow 7a_1'$	f	5.7565	46 429
$6a_1' \rightarrow 10e'$	a, xy	6.2071	50 063

[a] Abbreviations: a, allowed; f, forbidden.

ruthenium atom, and it too is essentially nonbonding, as shown in Figure 4.

The metal–metal bonding is essentially σ bonding, and the main contribution is made by the $7a_{1g}$ orbital, whose contours are shown in Figure 4. This orbital is also bonding in character toward the Ru–Cl_b σ bonds. However, the next lower a_{1g} orbital, $6a_{1g}$, also contributes significantly to the metal–metal σ bonding, as its contours in Figure 4 show. The LUMO is the $8a_{1g}$ orbital, and this is strongly antibonding not only in a metal–metal sense but also with respect to the Ru–Cl interactions. Its contours are shown in Figure 4.

Fenske–Hall Calculations. These were carried out on the $[RuCl_6]^{3-}$, $[Ru_2Cl_9]^{3-}$, and $[Ru_3Cl_{12}]^{4-}$ ions. The results obtained were in good qualitative accord with those obtained by the SCF–Xα–SW method. As usual, the energies obtained from the Fenske–Hall calculations were more spread out.

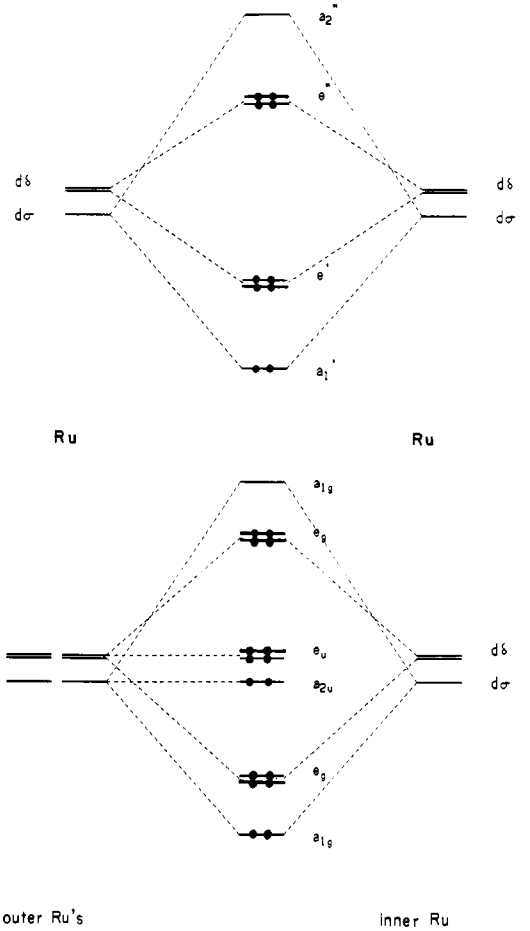

Figure 5. Qualitative energy level diagrams for the metal–metal interactions in $[Ru_2Cl_9]^{3-}$ (upper) and $[Ru_3Cl_{12}]^{4-}$ (lower).

There was, however, a generally good correspondence in the ordering of the levels.

The Fenske–Hall results were used to compute Mulliken atomic charges, and the results are shown in Table V. The charge distributions so obtained are physically very reasonable. In both $[Ru_2Cl_9]^{3-}$ and $[Ru_3Cl_{12}]^{4-}$ the bridging chlorine atoms have considerably lower charges than the terminal ones. This agrees with experimental results by X-ray photoelectron spectroscopy,[22] in which it is consistently found that the 2p binding energies of bridging chlorine atoms are greater (by 0.5–1.2 eV) than those for terminal chlorine atoms.

It is also notable that the charges for the central and outer ruthenium atoms are quite consistent with the formal oxidation numbers being +3 and +2, respectively, subject, of course, to the expectation based on the electroneutrality principle that actual metal atom charges remain less than 1+.

Discussion

Our principal objective in this work was to develop a reliable description of the Ru–Ru interactions in the $[Ru_2Cl_9]^{3-}$ and $[Ru_3Cl_{12}]^{4-}$ ions. We have also compared the computational results with the small amount of spectroscopic data available and shown that there is a reasonable measure of agreement. Let us now turn to a consideration of how the computational results may be interpreted in qualitative and chemically meaningful terms.

Let us consider first the dinuclear complex $[Ru_2Cl_9]^{3-}$. A qualitative attempt to describe the electronic structure of this closed-shell species might conveniently proceed as follows. We first consider each octahedral $RuCl_6$ portion of the dinuclear

(22) Ebner, J. R.; McFadden, D. L.; Tyler, D. R.; Walton, R. A. *Inorg. Chem.* **1976**, *15*, 3014.

Table IV. Upper Valence Molecular Orbitals of $[Ru_3Cl_{12}]^{4-}$

		% contribn[b]						% angular contribn[c]					
								Ru_1			Ru_2		
level[a]	energy, eV	Ru_1	Ru_2	Cl_t	Cl_b	INT	OUT	s	p	d	s	p	d
$12e_g$	−7.1173	5	53	16	17	7	1						100
$10e_u$	−7.2202	0	59	12	19	7	1						100
$11e_g$	−8.1571	53	6	29	3	7	0			100			
$8a_{1g}$	−9.3175	26	58	6	6	4	0			100			100
$7a_{2u}$	−9.8888	0	73	7	12	6	0						100
$9e_u$	−9.9427	0	75	4	14	7	0						100
$10e_g$	−9.9473	1	73	5	13	7	0						100
$9e_g$	−10.8310	72	2	15	4	6	0			100			
$7a_{1g}$	−11.0983	37	12	16	26	8	1			100		2	98
$2a_{2g}$	−11.5845	0	0	3	86	10	0						
$2a_{1u}$	−11.5916	0	0	2	87	10	0						
$8e_u$	−11.5926	0	0	5	84	10	0						
$8e_g$	−11.6363	3	0	4	81	11	0						
$6a_{2u}$	−11.8922	0	3	34	54	7	1						
$7e_g$	−12.1836	3	6	23	57	10	1						
$7e_u$	−12.2207	0	6	29	53	10	1						
$6a_{1g}$	−12.6121	17	17	5	50	10	1	2		98	8	3	89
$1a_{2g}$	−12.6745	0	0	86	3	11	0						
$6e_u$	−12.7167	1	8	36	44	10	0						
$1a_{1u}$	−12.9815	0	0	85	1	13	0						
$6e_g$	−12.9957	1	13	14	60	11	0					23	77
$5a_{2u}$	−13.0298	0	9	7	70	12	0						
$5a_{1g}$	−13.0566	1	8	5	73	12	0						
$5e_u$	−13.2565	0	5	55	27	11	1						
$4a_{2u}$	−13.7105	2	14	52	20	11	0				15	2	83
$5e_g$	−14.1113	7	17	46	19	11	0					2	98
$4e_u$	−14.1712	3	9	67	6	14	0						
$3a_{2u}$	−14.6551	3	10	68	9	10	0				81	8	11
$3e_u$	−14.7850	0	31	48	16	4	0						100
$4e_g$	−14.7937	14	16	56	5	9	0			100		3	97
$4a_{1g}$	−14.8617	10	7	60	9	13	0	27		73			
$3a_{1g}$	−15.3781	13	9	66	2	10	0	61		39			
$3e_g$	−15.5377	28	7	57	2	5	0			100			

[a] The HOMO is the $7a_{2u}$ level. [b] Abbreviations for charge distributions: INT = intersphere; OUT = outer sphere. [c] Listed only for levels with 10% or more Ru contributions. Ru_1 is the central ruthenium atom, and Ru_2 denotes the peripheral ruthenium atoms.

Table V. Mulliken Atomic Charges from Fenske–Hall Calculations

$RuCl_6^{3-}$		$Ru_2Cl_9^{3-}$		$Ru_3Cl_{12}^{4-}$ [a]	
Ru	1.077+	Ru	0.890+	Ru_1	0.266+
				Ru_2	0.890+
		Cl_b	0.379−	Cl_b	0.333−
Cl	0.680−	Cl_t	0.607−	Cl_t	0.674−

[a] Ru_1 is the central ruthenium atom, and Ru_2 denotes the peripheral ruthenium atoms.

unit using one 3-fold axis of the octahedron as the axis of quantization. The d_{xz} and d_{yz} orbitals are then the ones to be used in Ru–Cl σ bonding and the d_{z^2}, d_{xy}, and $d_{x^2-y^2}$ orbitals are those available to hold the metal d electrons and, to some extent, engage in Ru–Cl π interactions. When two such octahedra are fused on a common triangular face, to give a structure of D_{3h} symmetry, we obtain a structure in which the two d_{z^2} orbitals have σ character and can overlap to form σ and σ^* MO's, whose symmetry designations would be a_1' and a_2'', respectively. At the same time the $d_{xy}/d_{x^2-y^2}$ pairs will have δ character and can interact to form δ and δ^* MO's, with symmetry designations e′ and e″, respectively. For the $[Ru_2Cl_9]^{3-}$ ion, there are 10 electrons to occupy the MO's just discussed. A qualitative energy level diagram based on the above analysis is presented in Figure 5.

On this basis we correctly predict a closed-shell ground state with a net Ru–Ru bond order of unity. We also predict, in agreement with the SCF–Xα–SW and Fenske–Hall calculations, that the HOMO is an e″ orbital and the LUMO an a_2'' orbital. There is, however, a certain measure of *dis*agreement between the qualitative picture and the quantitative one. It was assumed, qualitatively, that, because of their directional properties, the d_{xz} and d_{yz} orbitals on the one hand and the d_{xy}, $d_{x^2-y^2}$ orbitals on the other would play rather different and independent roles: the former would be mainly engaged in Ru–Cl σ bonding and the latter mainly used to form the e′ and e″ molecular orbitals. There is, in fact, an almost complete hybridization of these two sets, with the result that both the e′ and e″ molecular orbitals are of very mixed character and not all of the pure δ character envisioned in the qualitative argument. In addition there is practically no difference in the energies of the 8e′ and 6e″ orbitals.

This high degree of mixing of the dπ and dδ type atomic orbitals under the D_{3d} symmetry of the chlorine atom arrangement does not, in fact, come as a surprise; it was already found in Ginsberg's calculation[10] on the $[Mo_2Cl_9]^{3-}$ ion. There is, in fact, excellent overall agreement between the $[Ru_2Cl_9]^{3-}$ and $[Mo_2Cl_9]^{3-}$ results.

Let us turn now to the $[Ru_3Cl_{12}]^{4-}$ ion. As already discussed briefly in the paper reporting the discovery of this ion,[15] a delocalized set of MO's, based on metal d orbitals, spanning the three metal atoms and occupied by 16 electrons should lead to equivalent Ru–Ru bonds of order $^1/_2$. The qualitative reasoning leading to this conclusion is the same, mutatis mutandis, as that outlined in detail above for $[Ru_2Cl_9]^{3-}$ and leads to the qualitative level diagram shown in Figure 5. Of the occupied orbitals shown, two are nonbonding, the two occupied e_g orbitals cancel each other, and what remains is a net two-electron, three-center bond. This is broadly similar to the result of the SCF–Xα–SW calculation, which gives a σ antibonding orbital ($8a_{1g}$) as the LUMO, and the top five occupied MO's are of the same types as those shown in the qualitative picture. The ordering of these five levels is not fully

in accord with the computational result, but the general picture is reasonable. Once again, a high degree of mixing of the dπ and dδ orbitals is revealed by the quantitative treatment. It is not, of course, surprising that since this occurred in $[Ru_2Cl_9]^{3-}$ it would continue to occur in the homologous $[Ru_3Cl_{12}]^{4-}$ ion.

The Ru–Ru distances in the $[Ru_2Cl_9]^{3-}$ and $[Ru_3Cl_{12}]^{4-}$ ions, 2.725 (3) and 2.805 (1) Å, respectively, are consistent with the formal bond orders of 1.0 and 0.5, respectively. Obviously, in structures of this kind where the metal–metal distance is a function of several other factors, especially the presence of bridging atoms, no simple quantitative correlation between metal–metal distance and metal–metal bond order alone is to be expected.

Acknowledgment. We thank the Robert A. Welch Foundation (Grant No. A-494) and the National Science Foundation for financial support. We are grateful to Dr. Jacques Darriet of the Laboratoire de Chemie du Solide du CNRS, Bordeaux, France, for samples of $Cs_3Ru_2Cl_9$ and to Drs. Douglas Carlson (Argonne National Laboratory) and Larry Falvello for help in recording spectra.

Registry No. $[RuCl_3]^{3-}$, 21595-26-6; $[Ru_2Cl_9]^{3-}$, 85865-40-3; $[Ru_3Cl_{12}]^{4-}$, 73412-78-9.

Contribution from the Department of Chemistry,
University of Western Ontario, London, Ontario N6A 5B7, Canada

Photoelectron Spectra and Bonding in Some Trimethylgold(III) Complexes

G. M. BANCROFT,* T. C. S. CHAN, and R. J. PUDDEPHATT*

Received December 15, 1982

The He I and He II photoelectron spectra of three Au(III) complexes, $[AuMe_3L]$ (L = PMe_3, PMe_2Ph, and $PMePh_2$), have been recorded in the gas phase. The spectra have been assigned with use of the previously assigned $[AuMe(PMe_3)]$ spectrum and the cross section differences between the He I and He II spectra. The Au $5d_{x^2-y^2}$ orbital is heavily involved in bonding—mainly to the phosphines. An attempt is made to assign the other Au 5d ionizations in a rather small (0.75 eV) range. Trends in binding energies for the three complexes indicate that the donor strength of the phosphines increases in the order $PMe_3 < PMe_2Ph < PPh_2Me$. A semiquantitative molecular orbital diagram for these complexes is constructed.

Introduction

Organogold(III) complexes, $[AuMe_3L]$ (L = phosphine), are found to undergo reductive elimination of ethane after dissociation of the phosphine ligand. Their catalytic properties in providing a pathway for the coupling between alkyllithium reagents and alkyl halides are well recognized.[1-3] The thermal stability of $[AuMe_3L]$ thus depends on the ease of dissociation of L, giving rise to gold(III) ($AuMe_3$) and gold(I) (AuMe) species as reactive intermediates. The presence of a strong Au–L bond, which is not readily cleaved, is responsible for the thermal stability of these complexes.[4]

As a continuation of our study of the bonding in gold phosphine complexes,[5,6] we report the He I and He II photoelectron spectra of three square-planar[7] $[AuMe_3L]$ (L = PMe_3, PMe_2Ph, $PMePh_2$) complexes. We had two major objectives in mind. First, we wanted to clarify the order of σ-donor ability of these ligands. The better σ-donor ligand is expected to increase the electron density at the metal, leading to a smaller binding energy for the Au 5d orbitals and the Au–C σ-bonding orbital.[8] It is also expected that the phosphine lone-pair orbital on the best donor will be stabilized the most upon complexation. Second, the overall molecular orbital diagram and in particular the role of the Au 5d orbitals in bonding are of considerably interest.[9] In our previous photoelectron study on $[AuMe(PMe_3)]$,[5] we confirmed that the Au $5d_{z^2}$ orbital is involved in bonding; such d involvement has been widely used to explain the high tendency of Au(I) to form linear complexes.[10-12] Using our assignment of the photoelectron spectra, we are able to comment on the Au 5d involvement in bonding and derive a semiquantitative molecular orbital diagram for our Au(III) complexes.

Experimental Section

The four gold(III) complexes, $[AuMe_3L]$ (L = PMe_3, $PPhMe_2$, PPh_2Me, and PPh_3), were prepared by using literature methods.[13-15] The complexes were then characterized with use of their characteristic melting points and ^1H NMR spectra.

The He I and He II photoelectron spectra of the complexes were run on our McPherson ESCA-36 photoelectron spectrometer using a hollow-cathode ultraviolet He lamp[16] and computer fitted to Lor-

(1) J. K. Kochi, "Organometallic Mechanisms and Catalysis", Academic Press, New York, 1978.
(2) J. Boor, "Ziegler-Natta Catalysis and Polymerization", Academic Press, New York, 1979.
(3) G. W. Parshall, *Science (Washington, D.C.)*, **208**, 1221 (1980).
(4) R. J. Puddephatt, *Gold Bull.*, **10** (4), 108 (1979).
(5) G. M. Bancroft, T. Chan, R. J. Puddephatt, and J. S. Tse, *Inorg. Chem.*, **21**, 2946 (1982).
(6) R. J. Puddephatt, T. Chan, and G. M. Bancroft, *Inorg. Chim. Acta*, 73, 83 (1983).
(7) J. Stein, J. P. Fackler, Jr., C. Paparizos, and H. W. Chen, *J. Am. Chem. Soc.*, **103**, 2192 (1981).
(8) J. Behan, R. A. W. Johnstone, and R. J. Puddephatt, *J. Chem. Soc., Chem. Commun.*, 444 (1978).
(9) S. Komiya, T. A. Albright, R. Hoffmann, and J. K. Kochi, *J. Am. Chem. Soc.*, **98**, 7255 (1976).
(10) L. E. Orgel, *J. Chem. Soc.*, 4186 (1958).
(11) C. K. Jørgensen and J. Pouradier, *J. Chim. Phys. Phys.-Chim. Biol.*, **67**, 124 (1970).
(12) P. Burroughs, S. Evans, A. Hamnett, A. F. Orchard, and N. V. Richardson, *J. Chem. Soc., Chem. Commun.*, 921 (1974).
(13) G. Galvin, G. E. Coates, and C. Parkin, *Chem. Ind. (London)*, 1628 (1959); G. E. Coates and C. Parkin, *J. Chem. Soc.*, 421 (1963).
(14) A. Johnson and R. J. Puddephatt, *J. Organomet. Chem.*, **85**, 115 (1975).
(15) R. J. Puddephatt and P. J. Thompson, *J. Chem. Soc., Dalton Trans.*, 1810 (1975).
(16) L. L. Coatsworth, G. M. Bancroft, D. K. Creber, R. J. D. Lazier, and P. W. M. Jacobs, *J. Electron Spectrosc. Relat. Phenom.*, **13**, 395 (1978).

0020-1669/83/1322-2133$01.50/0